

Vanadium(IV and V) Complexes Containing *SNO* (Dithiocarbonylhydrazone; Thiosemicarbazone) Donor Sets

Dongren Wang,^[a] Martin Ebel,^[a] Carola Schulzke,^[a] Cerstin Grüning,^[a]
Saroj K. S. Hazari,^[b] and Dieter Rehder^{*[a]}

Keywords: Vanadium / Thiosemicarbazones / Thiohydrazones / Sulfur coordination / Biomimetic compounds

The VO²⁺ complexes [VOCl(ONS)] (**3**) and [VO(ONS)'] (**4**), and the VO³⁺ complexes [VO(OEt)(ONS)'] (**5**) {ONS = (*R*)-salicylaldehyde thiosemicarbazone(1-), R = 5,6-C₄H₄ (**3a**) or 3-OMe (**3b**); (ONS)' = (*R*)-salicylaldehyde[benzylmercaptothiocarbonylhydrazone(2-)], R = H, (**4a/5a**) or 3-OMe (**4b/5b**)} have been prepared and characterised by IR, EPR, ¹H-, and ⁵¹V-NMR spectroscopy. In (*S*)-sBuOH, **4a** converts to [VO{(S)-OsBu}(ONS)'] (**5c**) and [VO(OH)(ONS)'] (or a condensation product thereof). Solutions of **5c** show three

⁵¹V NMR signals, two of which are due to two diastereomers. The EPR spectra of **3** and **4** in THF reveal the presence of octahedral species in solution. The crystal and molecular structures of complexes **3a**·OCMe₂, **5a**, and **5b** have been obtained, revealing basically a tetragonal pyramid, and coordination of the sulfur function in the thiocarbonyl (**3**) or enethiolate mode (**5**). The relevance of the compounds to bioinorganic aspects is addressed.

Introduction

Vanadium coordination chemistry has attracted increasing interest during the last few years, due to the model character of many vanadium complexes for the biological function of vanadium,^[1–5] the use of (oxo)vanadium complexes in oxidation and oxo transfer catalysis,^[6,7] and potential medicinal applications such as the treatment of diabetes types I (insulin deficiency) and II (insulin resistance).^[8,9] In its biogenic compounds, and in its interactions with biogenic ligand systems, vanadium coordinates to *O*, *N*, and *S* functions. Among the *O* functionalities are phenolate from tyrosine, as in the insulin-mimetic action of vanadium (possibly as a result of the inhibition of a protein tyrosine-phosphatase),^[10] as well as dopa and hydroxy-dopa of tunichrome fragments in the vanadocytes of certain species of *Ascididae* (sea squirts).^[11] The imine nitrogen atom of histidine is coordinated to vanadate(V) (HVO₄²⁻) in vanadate-dependent haloperoxidases from marine brown algae such as *Ascophyllum nodosum* (knobbed wrack),^[12] and from the mould *Curvularia inaequalis*,^[13,14] as well as to V^{IV} in the VFe cofactor of the *M* cluster of vanadium-nitrogenase from *Azotobacter*.^[15] In the latter case, the coordination sphere of vanadium is complemented by homocitrate and three bridging sulfides. Sulfur coordination, through cysteinate, has also been observed in vanadate-derivatised tyrosine phosphatase,^[16] and is likely to be the initiating step in redox inhibition by V^V of enzymes containing cysteine in their active centre.^[17] This process has been simu-

lated by the in vitro oxidation of thiolates to disulfides.^[18,19] As far as the use of vanadium-based catalyst systems in oxidation/oxygenation reactions is concerned, the conversion of sulfides (thioethers) RR'S to sulfoxides RR'S=O by peroxides is noteworthy, a process that is catalysed in vivo by vanadate-dependent peroxidases,^[20,21] and in vitro by vanadium complexes containing *ONO* donor sets,^[22–24] where *N* is an amine or imine function, and *O* a phenolic or alcoholic oxygen atom. The enantioselectivity of these reactions suggests an intermediate coordination of the sulfide to the vanadium centre, thus giving rise to an intermediate coordination sphere comprising *S*, *N*, and *O*.

Against this background, we are investigating vanadium complexes with *SNO* functional ligands such as thiosemicarbazones and mercaptothiocarbonylhydrazones with salicylaldehydes as the carbonyl component (Scheme 1). Sulfur coordination of these ligand systems occurs through the doubly bonded thio group in the case of the semicarbazones **1**, and through the thiolate group of the enethiol tautomer in the case of the hydrazones **2**, providing, in the latter case, rare examples^[25–30] of redox-stable V^V complexes with thiolate coordination. The hydrazones **2** with a “masked” thiolate function are employed advantageously for coordination to vanadium(V), since they resist the otherwise common oxidation of thiolates to disulfides by V^V.

Thio coordination to vanadium is additionally of interest with respect to the insulin-mimetic potential of vanadyl dithiocarbamates.^[31] More generally, metal complexes of thiosemicarbazones have also been discussed in the context of their antibacterial and antifungal properties.^[32,33]

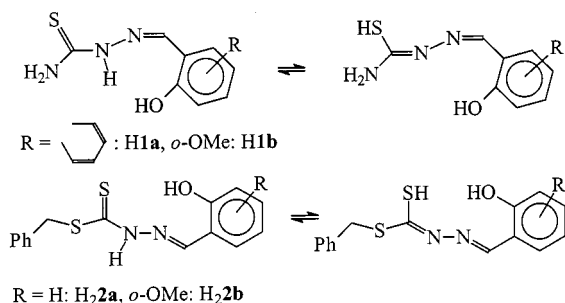
Results and Discussion

Preparation and Characteristics

The vanadium complexes were prepared as described by Equations (1) to (3) in THF [**3**; Equation (1)] and in eth-

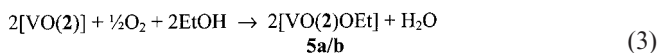
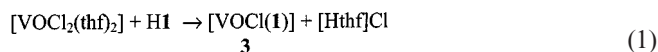
^[a] Institut für Anorganische und Angewandte Chemie, Universität Hamburg, 20146 Hamburg, Germany
E-mail: rehder@xray.chemie.uni-hamburg.de

^[b] Department of Chemistry, University of Chittagong, Chittagong, Bangladesh
E-mail: tapashi@ctgu.edu



Scheme 1

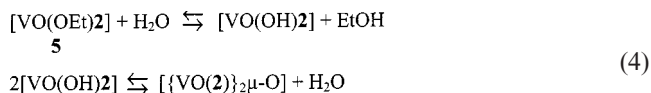
anol/water [**4**, Equation (2), and **5**, Equation (3)], respectively, under either an inert gas (**3** and **4**) or under aerobic conditions (**5**). An acetate buffer was used to capture the protons generated in Equation (2).



The green complexes **3a** and **3b** were isolated as the THF and water adducts (**3a**·³/₄THF and **3b**·¹/₂H₂O·¹/₂THF), respectively, the complexes **4a** and **4b** with varying amounts of solvent, viz. **4a**·EtOH, **4a**·¹/₄H₂O, and **4b**·H₂O. Crystals of **3a** were obtained as **3a**·OCMe₂ from acetone. Complexes **5a** and **5b** were free of coordinated solvent or solvent of crystallisation, and thus differ from the related hydrazone complex [VO(OMe)(SNO)''(HOMe)], where (SNO)'' is salicylaldehyde-thiobenzoylhydrazone.^[34] Spectroscopic data are summarised in Table 1 and Table 2. All of the complexes show the IR bands characteristic of ν(–HC=N–) (around 1600 cm^{–1}) and ν(V=O) (998–962 cm^{–1}), with the latter usually doubled; cf. Table 1. An additional sharp and intense band observed for the crystals of **3a**·OCMe₂ at 1696 cm^{–1} is assigned to ν(C=O) of acetone of crystallisation. The bathochromic shift with respect to free acetone is due to the involvement of the carbonyl group in H bonding interaction with N–NH and C–NH₂ of the semicarbazone

ligand, as identified by the X-ray structure analysis (see below). Complex **3a** still shows the ν(NH) (3276 and 3137 cm^{–1}) also present in the free ligand **1a** (3263 and 3165 cm^{–1}), indicating the coordination of the sulfur function in the thiocarbonyl form, a fact that is again corroborated by the structure determination. The corresponding ν(NH) for **1b** and **3b** are 3343 and 3167 cm^{–1}(**1b**), and 3291 and 3189 cm^{–1}(**3b**). The ν(C=S), 1192 in **1a** and 1185 cm^{–1} in **1b**, are slightly weakened on coordination, and thus experience a bathochromic shift to 1148 (**3a**) and 1162 cm^{–1}(**3b**). The complexes **4** and **5** show two resolved ν(C=N) bands, which we attribute to the presence of two C=N double bonds in the enethiolate framework of the hydrazone ligand (see the respective tautomeric form in Scheme 1).

The methine group is also clearly visible by its ¹H NMR feature (Table 2) of the diamagnetic complexes **5** (δ = 9.08); the methine proton resonances (δ = 7.98 in the free ligands **2**) are thus shifted to low (magnetic) field on coordination of the imine nitrogen atom. The protons of the methylene group of the benzyl substituent on the noncoordinating sulfur atom are only marginally affected. A feature of particular interest is the occurrence of two resonances, for the methylene and methyl protons of the ethyl group, in an intensity ratio of approximately 1:2 for uncoordinated ethanol and coordinated ethanolate, suggesting an equilibrium between ethoxide and hydroxo complex (or its condensation product) as depicted in Equation (4).



This situation is also reflected in the ⁵¹V NMR spectra, which show two resonances, separated by 51 ppm (**5a**) and 56 ppm (**5b**), with the less intense low-field signal corresponding to the hydroxo (or dimeric, μ-O-bridged) form. This assignment is carried out on the basis of the spectrum obtained after treatment of **4a** with (S)-sBuOH, which gives rise to the formation of [VO{(S)-OsBu}2a] (**5c**) with two centres of chirality (V and C_a of the butoxide group) in equilibrium with [VO(OH)2a]. Of the two resonances, the less intense one at δ = –347 is a singlet belonging to the

Table 1. Selected IR, δ(⁵¹V) and EPR data

	ν(N=CH) ^[a]	ν(V=O) ^[a]	δ(⁵¹ V) ^[b]	g ₀	A ₀ ^[c]
3a	1618	995 ^[d]		1.979	98.7, 101.0 ^[e] (THF)
3b	1605	998/973 ^[f]		1.971	94.3, 100.7 (CH ₂ Cl ₂)
4a	1603, 1588	988, 966		1.972	93.7, 100.9 ^[g] (THF)
4b	1603, 1590	991, 977		1.98	99.8 ^[h]
5a	1602, 1590	984, 962 sh	–348 ^[i] , –399	1.98	99.6
5b	1600, 1589	985, 976 sh	–340 ^[i] , –396		
5c	1601, 1590	986	–347 ^[i] , –411/–414		

[a] In KBr; in cm^{–1}. – [b] In CDCl₃. – [c] A in 10^{–4} cm^{–1}. – [d] In THF solution, the ν(V=O) is at 976 cm^{–1}. – [e] Two components (I and 2, not resolved in g) are present; A₀ = 93.7·10^{–4} cm^{–1} corresponds to the main component I. Parameters under anisotropic conditions (100 K): g values (obtained from a fitting procedure) are g_{xy}^(I) = 1.99, g_z^(I) = 1.956; g_{xy}⁽²⁾ = 1.981, g_z⁽²⁾ = 1.950; A_{xy}^(I) = 60, A_z^(I) = 161; A_{xy}⁽²⁾ = 65, A_z⁽²⁾ = 173·10^{–4} cm^{–1}. Cf. also Figure 1 and Equation (5). – [f] Broad resonance with two maxima. – [g] The ratio of components I and 2 is reversed with respect to **3a**, i.e. the smaller A corresponds to the minor species. Anisotropic coupling constants of main component: A_z⁽²⁾ = 160, A_{xy}⁽²⁾ = 61·10^{–4} cm^{–1}. – [h] g_z = 1.96, g_{xy} = 1.99; A_z = 176.5, A_{xy} = 63.4·10^{–4} cm^{–1}. – [i] This signal corresponds to [VO(SNO)OH] or [{VO(SNO)}₂μ-O].

Table 2. $\delta(^1\text{H})$ NMR spectroscopic data

Ligand ^[a]	–NH–	–N=CH–	PhCH ₂ S–	–OCH ₃	–OCH ₂ CH ₃	–OCH ₂ CH ₃
2a	9.98	7.98	4.60			
2b	9.89	7.98	4.56	3.91		
5a	–	9.08	4.47		1.25, 1.63 ^[b]	3.72, 5.42 ^[b]
5b	–	9.08	4.48	3.95	1.24, 1.64 ^[b]	3.75, 5.45 ^[b]

^[a] In CDCl₃. For the ligands **1a** and **1b**, see Exp. Sect. – ^[b] Intensity ratio ca.1:2; the first signal corresponds to free ethanol.

butoxide-free complex, while the more intense to higher field is doubled and belongs to **5c**. The separation between the two components of this signal, $\delta = -411.3$ and -414.2 , is within the range expected for the signal splitting for a vanadium compound being present as two diastereomeric pairs of enantiomers.^[35,36] The ^{51}V chemical shifts are in the range expected for a donor set containing one sulfur function, i.e. to low field by about 150 to 200 ppm with respect to complexes with $O_N N_V$ donor sets.^[37]

The EPR spectrum of crystals of **3a**·OCMe₂ dissolved in THF exhibits the isotropic eight-line pattern typical of VO²⁺ complexes [$S = 1/2$, $I(^{51}\text{V}) = 7/2$]. Along with the main species in this spectrum, characterised by a hyper-fine coupling constant $A_0 = 93.7 \cdot 10^{-4} \text{ cm}^{-1}$, there is a second species with a rather high value ($A_0 = 101.0 \cdot 10^{-4} \text{ cm}^{-1}$). This situation is also revealed by the anisotropic spectrum in frozen THF solution (Figure 1), which is a superposition of the parallel (z) and perpendicular (xy) parts of the main (1) and the minor component (2). The A_z values are $A_z^{(1)} = 161 \cdot 10^{-4}$ and $A_z^{(2)} = 173 \cdot 10^{-4} \text{ cm}^{-1}$. Based on the additivity relationship $A_z = \sum n_i A_{z_i}$ (n_i denotes the nature of the four equatorial ligand functions, and A_{z_i} are the corresponding contributions to A_z),^[38] a value of $161 \cdot 10^{-4} \text{ cm}^{-1}$ is in agreement with an equatorial *ClONS* donor set in **3a**, while a value of $173 \cdot 10^{-4} \text{ cm}^{-1}$ should indicate addition of an oxygen-functional ligand L in solution, such as THF, possibly accompanied by a rearrangement of the tridentate ligand so as to place the sulfur donor atom into an axial position.

Taking 45.7 and $33.9 \cdot 10^{-4} \text{ cm}^{-1}$ as the contributions of a relatively weak O donor such as THF^[39] and the thiocarbonyl function, respectively, a calculated value of $A_z^{(2)} = 172.8 \cdot 10^{-4} \text{ cm}^{-1}$ is obtained, in very good agreement with the found coupling constant of $173 \cdot 10^{-4} \text{ cm}^{-1}$. We hence suggest an equilibrium as depicted in Equation (5), where species 1 is represented by **3a** and species 2 by *trans*-**3a(L)**, where *trans* denotes the position of S in the axial position (*trans* to the doubly bonded oxo ligand). In THF solutions, L would presumably be THF.

Since the same pattern arises in the isotropic spectrum of a solution of **3a**·OCMe₂ in CH₂Cl₂, where the compound is but sparingly soluble, L appears to be acetone in this solvent. In principal, the EPR of the vanillin derivative **3b** compares well with that of **3a**, in that there are two components 1 and 2 present in the spectrum. The ratio is, however inverse, i.e. compound 2 corresponding to the species with the larger coupling constant, **3b(L)**, is the major component. The *A*₀ and *A*_z values for **4a** and **4b** are somewhat larger (Table 1) than those for the tetragonal-pyramidal spe-

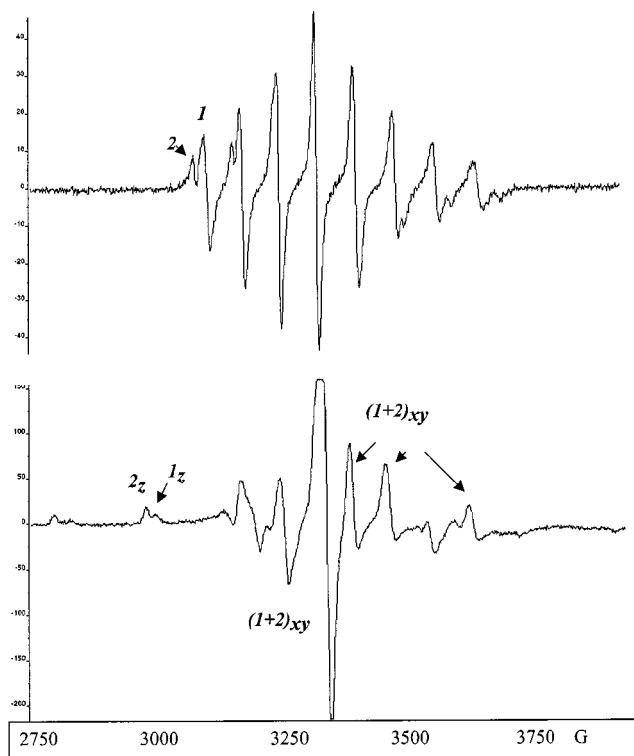
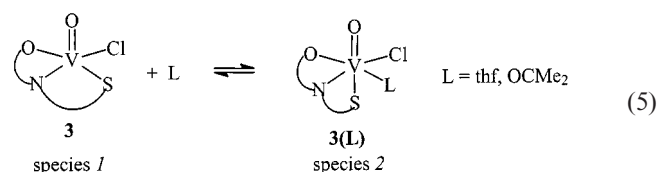


Figure 1. EPR spectrum of **3a** in THF solution at room temperature (top) and at 100 K; the z (parallel) and xy (perpendicular) components are indicated, as are the two species 1 and 2 present in solution; cf. Equation (4)

cies **1** of **3a** and **3b**, in accord^[40] with an octahedral coordination in solution and the equatorial plane dominated by strongly electronegative ligand functions in the case of **4**, which thus corresponds to **3(L)**. Again, the sixth position in the coordination polyhedron of THF solutions of **4** is supposed to be occupied by THF.



Structure Descriptions

Selected bond lengths and bond angles are given in Table 3. In the V^{IV} (VO²⁺) thiosemicarbazone complex **3a**, vanadium is basically in a tetragonal-pyramidal environment (Figure 2) with the doubly bonded oxo group O1 of the vanadyl moiety in the apical position, and the chloro

ligand, O2, N1, and S3 of the tridentate thiosemicarbazone ligand in the plane. There is a sizeable distortion towards a trigonal bipyramid, quantified by a τ value of 0.28, where τ is defined by $\tau = [(O2-V-N1) - (O3-V-S2)]/60$; $\tau = 0$ for ideal tetragonal pyramids, and $\tau = 1$ in the case of an ideal trigonal bipyramid. The S3–C12 bond [1.708(3) Å] is significantly shorter than in most structurally characterised Ni and Cu complexes with comparable ligands (ca. 1.73–1.76 Å^[39,41–44]), indicating coordination of the ligand through a thiocarbonyl rather than through an enthiolate in the case of **3a**, and is thus in agreement with thiosemicarbazones coordinated to early transition metals such as Cr^[45] and Mo.^[46] This view is corroborated by the localisation of the hydrogen atom on the nonbonding N2, which is linked by an intermolecular hydrogen bond to the carbonyl oxygen atom O3 of acetone of crystallisation; $d(O3\cdots H-N2) = 2.154$ Å. Further intermolecular hydrogen bonds exist between the hydrogen atoms on the primary amine group (N3) and O3 [$d(O3\cdots H-N3) = 2.02$] and the phenolate oxygen atom O2 [$d(O2\cdots H-N3) = 2.019$ Å]. The hydrogen bonding network is shown in Figure 2 (bottom).

Other bonding parameters within the ligand system are comparable to those in thiosemicarbazone complexes of other metals.^[38–46] The bond lengths between the vanadium centre and the three ligand functions also compare to those of the vanadium-ONS complex [V(nap-amtph)₂], where nap-amtph is the Schiff base formed between *o*-hydroxynaphthaldehyde and *o*-aminothiophenol,^[47] and to

[V(mpg)*o*-phen] [H₃mpg = *N*-(2-mercaptopropionyl)glycine]. In all these complexes [as in the hydrazone complexes **5** (see below)] the V–S bond lengths [**3a**: 2.358(1), [V(nap-amtph)₂]: 2.306(2) and 2.351(2), [V(mpg)*o*-phen]: 2.3820(14) Å] fall at the short end of the range for $d(V-S)$;^[47–49] they are also significantly shorter than in the complex [VO(H₂O)L], where H₂L is thiosemicarbazone-diacetate; [$d(V-S) = 2.435$, $d(V-N) = 2.362$ Å].^[50] On the other hand, V–S bonds in V^V complexes containing the tetrafunctional trithiolate N(CH₂CH₂S[−])₃ are still shorter (averaging around 2.25 Å^[29,30]) than in the aforementioned complexes with ONS donor sets. The V–Cl bond in **3a** [2.341(1) Å] again compares to that in other chlorovanadium complexes.^[35,51,52]

A tetragonal pyramid is also the basic structure for the V^V (VO³⁺) thiohydrazone complexes **5a** and **5b** (Figure 3), in which the chloro ligand of the V^{IV} complex **3a** is replaced by an ethanolate moiety, and the tridentate ONS acts as a dianionic ligand. The vanadium ion is 0.49 (**5a**) and 0.52 Å (**5b**) above the plane spanned by S2, N1, O2, and O3 (i.e. the tridentate ligand and the ethoxy group). The distortion towards a trigonal bipyramid compares with that of **3a**, i.e. $\tau = 0.28$ (**5a**) and 0.27 (**5b**). As expected for enthiolate (**5**) vs. thiocarbonyl coordination (**3**), the bond lengths $d(S-C2)$ in **5** are substantially longer than $d(S-C12)$ in **3a**, the $d(N2-C2)$ in **5** substantially shorter than $d(N2-C12)$ in **3a** (Table 3). In line with this view are the bond angles at N2: (N1–N2–C12) = 118.7(2)° in **3a** is close to the tet-

Table 3. Selected structure parameters

	[VOCl(1a)], 3a	[VO(OEt)(2a)], 5a	[VO(OEt)(2b)], 5b ^[a]
<i>Bond lengths [Å]</i>			
V–Cl	2.341(1)		
V=O (V1–O1)	1.590(2)	1.594(3)	1.608(6)
V–O(phenolate)	1.914(2) (V–O2)	1.828(3) (V–O3)	1.859(4)
V–O(ethanolate)		1.754(3) (V–O2)	1.771(6)
V–S	2.358(1)	2.343(2) (V–S2)	2.345(3)
V–N1	2.087(3)	2.152(3)	2.098(5)
S(coord.)–C12/2	1.708(3) (S–C12)	1.731(4) (S2–C2)	1.750(6)
N2–C12/2	1.334(4) (N2–C12)	1.290(6) (N2–C2)	1.289(7)
N1–N2	1.391(3)	1.393(5)	1.402(6)
N1=CH–	1.303(4) (N1–C11)	1.287(6) (N1–C3)	1.301(7)
O(phenolate)–C	1.334(4) (O2–C1)	1.344(6) (O3–C6)	1.339(7)
S1–C2		105.0(2) (O1–V–O2)	101.6(4)
<i>Bond angles [°]</i>			
O1–V–Cl	105.78(9)		
O1–V–O(phenolate)	111.03(11) (O1–V–O2)	108.5(2) (O1–V–O3)	110.1(4)
O1–V–O(ethanolate)		105.0(2) (O1–V–O2)	101.6(4)
O1–V–N1	99.57(11)	95.5(2)	95.0(3)
O1–V–S	110.58(9)	107.30(14) (O1–V–S2)	107.0(2)
Cl–V–O(phenolate)	89.71(7)		
Cl–V–S	87.15(3)		
O(eth.)–V–O(phen.)		99.4(2) (O2–V–O3)	95.2(3)
O(ethanolate)–V–S2		87.14(13) (O2–V–S2)	86.1(2)
O(phenolate)–V–S	137.50(7)	140.39(13) (O3–V–S2)	140.67(16)
N1–V–S	80.69(7)	77.28(11) (N1–V–S2)	78.81(15)
S–C(carbonyl)–N2	120.7(2) (S–C12–N2)	127.7(3) (S2–C2–N2)	125.6(4)
C(carbonyl)–N2–N1	118.7(2) (C12–N2–N1)	112.5(3) (C2–N2–N1)	112.2(5)
N2–N1=CH	116.3(2) (N2–N1–C11)	112.2(3) (N2–N1–C3)	112.4(5)
N1=CH–C(Ph)	124.1(3) (N1–C11–C10)	125.3(4) (N1–C3–C11)	125.0(6)
V1–O(phen.)–C(Ph)	126.78(18)	132.5(3) (V1–O3–C6)	132.0(4)
C2–S1–C1		102.2(2)	102.3(3)

[a] Same numbering scheme as for **5a**.

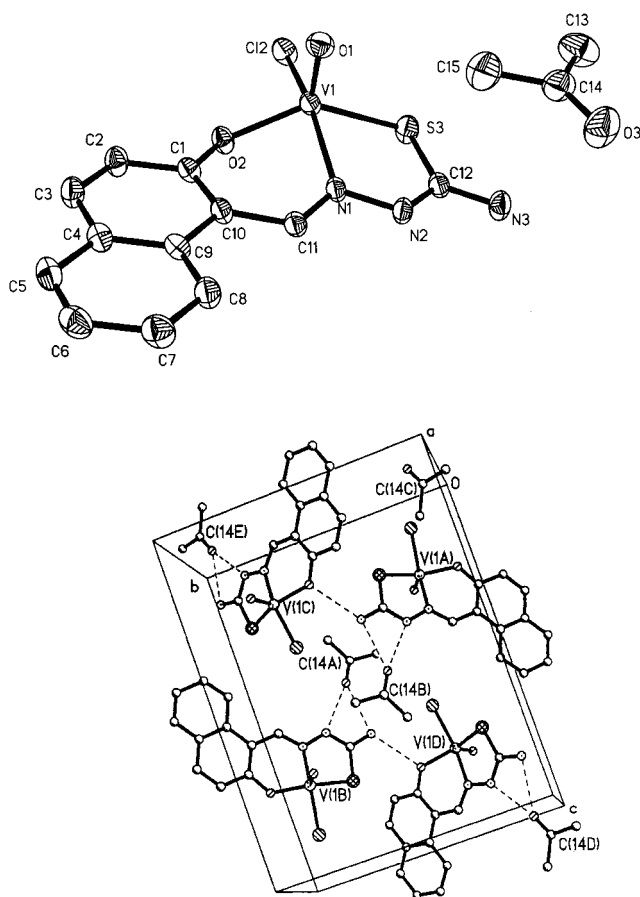


Figure 2. ORTEP plot (at the 50% probability level) and numbering scheme of **3a**·acetone (top), and a representation of the unit cell (bottom) showing the hydrogen bonding network (dashed lines)

rahedral angle, while the angles (N1–N2–C2) = 112.5(3) (**5a**) and 112.2(5)° (**5b**) are close to that for trigonal planar geometry. The exchange of chloride in **3a** for ethanolate in **5** does not effect $d(\text{V}–\text{N}1)$ *trans* to the negatively charged ligand, while the V–O(phenolate) bond is clearly shorter in **5** than in **3a**, and also shorter than in other structurally characterised early transition metal (Cr and Mo) complexes with a similar donor set,^[45,46] or in Schiff base oxovanadium complexes with a salicylaldehyde moiety.^[53] The reason for these unprecedentedly short V–O(phenolate) bonds, which approach the lengths otherwise observed with V–O(alcoholate) bonds [1.80 to 1.74 Å,^[54] cf. also the respective data for $d(\text{V}–\text{O}2)$ in Table 3], may be traced back to a strengthening of this bond as a result of comparatively weak bonding interaction between V^{V} and the soft thiolate opposite the hard phenolate oxygen.

The bicyclic system formed between the vanadium centre and the tridentate ligand is slightly folded along the V–N1 axis: The angles between the planes V–O3–C6–C11–C3–N1 and V–N1–N2–C2–S2 amount to 16.92(15) (**5a**) and 20.41(22)° (**5b**). The planes by themselves are not ideal, with the largest deviations encountered with V1 (–0.228) and O3 (0.252 Å) in the plane V–O3–C6–C11–C3–N1 of **5a**. Despite of the similarities between **5a** and **5b**, the only difference being the presence

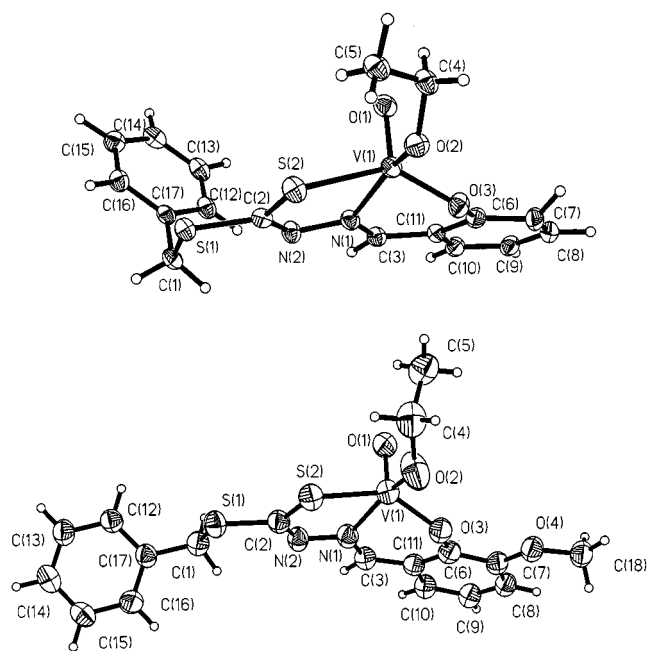


Figure 3. ORTEP plots (50% probability level) and numbering schemes for **5a** (top) and **5b** (bottom)

of a methoxy substituent on the aldehyde component in **5b**, the arrangement of the outer spheres of these complexes exhibits specific differences; Figure 3. While, in **5b**, the benzyl moiety stretches towards the periphery and the ethanolate is bent off the V=O group, the benzyl and ethoxide groups in **5a** are arranged so as to provide a large open cavity approximately 8.3 Å across.

Experimental Section

Starting materials were obtained from commercial sources [thiosemicarbazone, salicylaldehyde, 2-hydroxynaphthalenecarbaldehyde, *o*-vanillin, hydrazine hydrate (99–100%), and oxovanadium sulfate pentahydrate]. $[\text{VOCl}_2(\text{thf})_2]$ was prepared according to a literature procedure.^[55]

Physical Measurements: IR spectra were obtained as KBr pellets with a Perkin–Elmer spectrometer 1720 FT. – NMR spectra were recorded with a Bruker AM 360 or Varian Gemini 200 BB spectrometer with the usual spectrometer settings. All $\delta(^{51}\text{V})$ values are referenced against VOCl_3 . – EPR spectra were measured with a Bruker ESP 300E spectrometer at 9.74 GHz in 1–5 mm solutions. ^1H and ^{51}V NMR, EPR, and selected IR data for the complexes are collated in Table 1 and Table 2 in the Discussion. – X-ray structure analyses were carried out in the $\theta/2\theta$ scan mode with an Enraf–Nonius CAD4 diffractometer with monochromated (graphite monochromator) $\text{Cu}-K_\alpha$ irradiation ($\lambda = 1.54178$ Å). The hydrogen atoms on N2 and N3 of **3a**·OCMe₂ were located; all other hydrogen atoms were placed into calculated positions and included with isotropic displacement factors in the last cycles of the structure refinements. The program packages SHELXS 86^[56] and SHELXL 93^[57] were used throughout. Absorption corrections (DI-FABS) were carried out. Crystal data and data for the structure solutions and refinements are collated in Table 4. Crystallographic data (excluding structure factors) for the structures reported in this

Table 4. Structure and refinement parameters

	3a·OCMe₂	5a	5b
Empirical formula	C ₁₅ H ₁₆ ClN ₃ O ₃ SV	C ₁₇ H ₁₇ N ₂ O ₃ S ₂ V	C ₁₈ H ₁₉ N ₂ O ₄ S ₂ V
Molecular mass [g mol ⁻¹]	404.76	412.39	442.41
Temperature [K]	173(2)	293(2)	173(2)
Crystal system	monoclinic	triclinic	triclinic
Space group	<i>P</i> 2 ₁ / <i>c</i>	<i>P</i> 1	<i>P</i> 1
<i>a</i> [Å]	7.7413(17)	10.069(2)	8.319(12)
<i>b</i> [Å]	13.219(2)	10.170(4)	10.515(4)
<i>c</i> [Å]	17.044(4)	10.241(4)	12.244(13)
α [°]		90.87(3)	72.51(7)
β [°]	98.28(2)	115.56(3)	71.02(11)
γ [°]		107.63(3)	81.30(6)
Cell volume [Å ³]	1725.9(7)	888.6(3)	964.3(18)
<i>Z</i>	4	2	2
Density (calcd.) [g cm ⁻³]	1.558	1.541	1.524
Absorption coeff. [mm ⁻¹]	7.53	7.03	6.56
<i>F</i> (000)	828	424	456
Crystal size [mm]	0.6 × 0.3 × 0.2	1.1 × 0.3 × 0.1	0.9 × 0.25 × 0.1
θ range [°]	4.25–76.32	4.63–76.39	5.08–76.36
Index ranges	–9 < <i>h</i> < 3 0 < <i>k</i> < 16 –21 < <i>l</i> < 21	–11 < <i>h</i> < 12 –12 < <i>k</i> < 12 –12 < <i>l</i> < 5	0 < <i>h</i> < 10 –13 < <i>k</i> < 13 –14 < <i>l</i> < 15
Reflections collected	3937	3986	4387
Unique reflections	3626	3727	4046
<i>R</i> (int)	0.0307	0.0324	0.0366
Number of param.	233	295	247
<i>R</i> indices, <i>I</i> > 2 σ (<i>I</i> ₀):			
<i>R</i> 1, <i>wR</i> 2	0.0561, 0.1446	0.0809, 0.2125	0.0805, 0.2226
<i>R</i> indices, all data	0.0650, 0.1577	0.0913, 0.2259	0.1378, 0.2606
<i>R</i> 1, <i>wR</i> 2			
Diff. peak/hole [e Å ⁻³]	1.205/–1.224	1.772/–1.040	0.680/–0.525

paper have been deposited with the Cambridge Crystallographic Data Centre as supplementary publication no. CCDC-152692 (**5b**), -152693 (**5a**) and -152694 (**3a·OCMe₂**). Copies of the data can be obtained free of charge on application to CCDC, 12 Union Road, Cambridge CB2 1EZ, UK [Fax: int. code + 44-1223/336-033; E-mail: deposit@ccdc.cam.ac.uk].

2-Hydroxynaphthalene-1-carbaldehyde Thiosemicarbazone (H1a), and 6-Methoxysalicylaldehyde Thiosemicarbazone (H1b): These ligands were synthesised in analogy to the procedure of Poruhit et al.^[58] For the preparation of **H1a**, a hot solution of thiosemicarbazone (2.25 g, 25 mmol) in 20 mL of ethanol was treated with 2-hydroxynaphthalenecarbaldehyde (4.31 g, 25 mmol) in 20 mL of ethanol, and the mixture was gently heated under reflux for 4 h. It was then cooled down to room temp., the precipitate collected by filtration, washed with ethanol and dried in vacuo. Yield 3.44 g (60%). – C₁₂H₁₂N₃OS (246.31): calcd. C 58.76, H 4.52, N 17.14; found C 58.44, H 4.63, N 17.09. – **H1b** was obtained with a yield of 7.14 g (74%) in an analogous manner from thiosemicarbazone (4.50 g, 50 mmol, dissolved in 20 mL of ethanol) and *o*-vanillin (7.60 g, 50 mmol, dissolved in 10 mL of ethanol) after 2 h of heating under reflux. – C₉H₁₁N₃O₂S (225.27): calcd. C 47.99, H 4.90, N 18.66; found C 47.60, H 5.22, N 18.21. – ¹H NMR: δ (THF) [multiplicity, *J* Hz] = 10.71 and 10.57 (NH, NH₂); 9.03 (N=CH); 8.15 [d, 8.5], 7.807 [d, 9.0] and 7.79 [dd, 6.8], 7.51 [tt, 7.7 and 1.3], 7.37 [tt, 7.1], 7.14 [d, 9.0] (aromatic H).

Salicylaldehyde- and 6-Methoxysalicylaldehyde [(Benzylmercapto)-thiocarbonyl]hydrazones (H₂2a and H₂2b): The ligands were prepared by condensation of benzylmercaptothiocarbonylhydrazine (benzyl dithiocarbazate) and salicylaldehyde or *o*-vanillin.^[59] Benzylmercaptothiocarbonylhydrazine (3.97 g, 20 mmol) and salicylaldehyde/vanillin (2.0 mL/3.05 g, 20 mmol), dissolved in 100/150 mL of ethanol, were heated under reflux for 90 min. The ligands separated in the form of pale yellow crystals on cooling the

solution to room temp. Yield for **H₂2a/H₂2b** after recrystallisation from ethanol: 4.65/4.31 g (75/65%). The precursor benzylmercaptothiocarbonylhydrazine was prepared as follows: KOH (22.9 g) was dissolved in 140 mL of 90% ethanol and treated with 20 mL of hydrazine hydrate. The mixture was cooled in an ice bath to 8–10 °C, and 25 mL of CS₂ was added dropwise with stirring. The orange-yellow oil that formed was separated with a separating funnel and redissolved in 120 mL of precooled 40% ethanol, and the solution placed in an ice bath. Benzoyl chloride (50 mL) was then added with vigorous stirring. The ester separated as a white solid, which was filtered off and recrystallised from toluene and ethanol to yield 11.11 g of dry product. Additional 4.46 g of the compound was obtained by adding water to the filtrate and workup of the resulting precipitate. Overall yield 19%.

[VOCl(1a)] (3a) and [VOCl(1b)] (3b). – **3a:** To a stirred solution of **H1a** (0.25 g, 1.0 mmol) in 20 mL of THF was added [VOCl₂(thf)₂] (0.28 g, 1.0 mmol) in 15 mL of THF. The resulting green solution was stirred at room temp. for 2 h. The green compound that separated was filtered off, washed with THF and then with *n*-pentane, and dried in vacuo. Yield 0.19 g (50%). – Analysis for **3a**·³/₄THF: C₁₂H₁₀ClN₃O₂SV·³/₄THF (400.76): calcd. C 44.96, H 4.02, N 10.48, V 12.71; found C 44.74, H 4.26, N 10.32, V 12.68. – IR (KBr): $\tilde{\nu}$ /cm⁻¹ = 3131, (NH), 1618 (C=N), 1541 (NH), 995 (V=O). – Crystals of **3a**·acetone suitable for the X-ray analysis were obtained by allowing an acetone solution of **3a** to slowly concentrate at room temperature. – **3b** was prepared in an analogous manner to **3a** from [VOCl₂(thf)₂] (0.28 g, 1.0 mmol) and **H1b** (0.23 g, 1.0 mmol) with a yield of 0.24 g (70%). – C₉H₁₀ClN₃O₃SV·¹/₂THF·¹/₂H₂O (371.70): calcd. C 35.53, H 4.07, N 11.30; found C 35.38, H 4.06, N 11.14. – IR (KBr): $\tilde{\nu}$ /cm⁻¹ = 3186 (NH), 1605 (C=N), ca. 980 (V=O).

[VO(2a)]·EtOH (4a·EtOH): The hydrazone **H₂2a** (0.79 g, 2.61 mmol), vanadyl sulfate (0.66 g, 2.61 mmol) and sodium acet-

ate trihydrate (0.71 g, 5.2 mmol) were dissolved in 60 mL of ethanol and stirred under N_2 over night. The green solution was then treated dropwise with 150 mL of N_2 -saturated water. A green precipitate of **4a**·EtOH formed, which was filtered off, washed with water and pentane, and dried in vacuo. Yield 0.75 g (70%). — $C_{17}H_{18}N_2O_3S_2V$ (413.40): calcd. C 49.39, H 4.39, N 6.78; found C 49.43, H 4.59, N 6.74. — IR (KBr): $\tilde{\nu}/cm^{-1}$ = 3057/3026 (ArH), 2972 (CH_2), 1625, 1603/1588 (HC=N), 1546 (Ph—C=N), 1280, 1029, 985/967 (V=O), 823, 754, 698 [$\delta(CH)$], 631, 567, 519, 459.

[VO(2a)]· $\frac{1}{4}$ H $_2$ O (4a· $\frac{1}{4}$ H $_2$ O): To a suspension of **H $_2$ 2a** (0.76 g, 2.5 mmol) and sodium acetate trihydrate (0.68 g 5 mmol) in 60 mL of ethanol was added (under N_2) dropwise within 5 min a solution of oxovanadium sulfate pentahydrate (0.64 g (2.5 mmol) in 30 mL of water, and the mixture stirred at room temp. until all of the **H $_2$ 2a** had been taken up by the green solution (ca. 90 min). Water (90 mL) was added dropwise to precipitate **4a** as a microcrystalline product, which was filtered off, washed thoroughly with water followed by a few mL of pentane, and dried in vacuo. According to the elemental analysis, the green product contained $\frac{1}{4}$ mol percent of water. — $C_{15}H_{12}N_2O_2S_2V \cdot \frac{1}{4}H_2O$ (371.84): calcd. C 48.45, H 3.39, N 7.53; found C 48.52, H 3.50, N 7.58. — The IR shows essentially the same features as that of **4a**·EtOH.

[VO(2b)]·H $_2$ O (4b·H $_2$ O): The hydrazone **H $_2$ 2b** (1.66 g, 5.0 mmol), vanadyl sulfate (1.28 g, 5 mmol), and sodium acetate trihydrate (1.37 g, 10.0 mmol) were dissolved in 50 mL of ethanol and stirred under N_2 overnight. The solution initially turned orange-brown, and a brown precipitate formed. (In more dilute solutions, the amount of precipitate that formed decreased, and the solution exhibited a brown-green colour.) To this suspension, 100 mL of water, degassed and saturated with N_2 , was added dropwise and with stirring. The precipitate turned green; it was filtered off, washed with water and pentane, and dried in vacuo. Yield 1.40 g (69%). — $C_{16}H_{16}N_2O_4S_2V$ (415.38): calcd. C 46.27, H 3.88, N 6.74; found C 46.65, H 3.76, N 6.77. — IR (KBr): $\tilde{\nu}/cm^{-1}$ = 3084, 3061, 3030 (ArH), 2848 (OMe), 1602/1686 (HC=N), 1553 (Ph—C=N), 1299, 1255, 1110, 991/977 (V=O), 768, 735, 693, 606, 515.

[VO(OEt)2a] (5a), and [VO(OEt)2b] (5b): Complex **4a**·EtOH or **4b**·H $_2$ O was heated under reflux in ethanol for 3–4 h (no inert gas). The brown to dusky brown products were separated and dried in vacuo. — **5a**: $C_{17}H_{18}N_2O_3S_2V$ (413.40): calcd. C 49.39, H 4.39, N 6.78; found C 49.43, H 4.59, N 6.74. — IR (KBr): $\tilde{\nu}/cm^{-1}$ = 3023 (ArH), 2974, 2922, 2860 (CH_2), 1602/1590 (HC=N), 1550 (Ph—C=N), 1275, 1028, 1004, 984/962 (V=O), 914, 909, 834, 765, 696 [$\delta(CH)$], 645, 537, 519, 459. — **5b**: $C_{18}H_{19}N_2O_4S_2V$ (442.42): calcd. C 48.87, H 4.33, N 6.33; found C 45.99, H 4.14, N 6.45. — IR (KBr): $\tilde{\nu}/cm^{-1}$ = 3028 (ArH), 2983, 2934, 2832 (CH_2), 1600/1589 (HC=N), 1555 (Ph—C=N), 1285, 1257, 1227, 1108, 985/976 (V=O), 969, 776, 738, 699, 605, 447. — Black-brown rhombohedral crystals of **5a** and **5b** suitable for an X-ray diffraction analysis were obtained by allowing hot ethanol solutions to slowly cool down to room temperature.

Acknowledgments

This work was supported by the Deutsche Forschungsgemeinschaft (grant Re 431/13–3), the Fonds der Chemischen Industrie, the Deutsche Akademische Austauschdienst (stipend for S. K. S. H.), and a fellowship donated by the P. R. China (D. W.). We thank Prof. T. Kabanos, University of Ioannina, for his support in interpreting the EPR spectra.

- [1] *Vanadium Compounds, Chemistry, Biochemistry and Therapeutic Applications* (Eds.: A. S. Tracey, D. C. Crans), ACS Symp. Ser. 711, 1998.
- [2] *J. Inorg. Biochem.* **2000**, 80 (Special Issue on Biological Aspects of Vanadium; Guest Eds.: D. Rehder, V. Conte).
- [3] *Vanadium and Its Role in Life* (vol. 31 of *Metal Ions in Biological Systems*; Eds.: H. Sigel, A. Sigel), Marcel Dekker, New York, 1995.
- [4] D. Rehder, *Coord. Chem. Rev.* **1999**, 182, 297.
- [5] *Vanadium in the Environment* (Ed.: J. O. Nriagu), Wiley, New York, 1998.
- [6] T. Hirao, *Chem. Rev.* **1997**, 97, 2707.
- [7] J. W. C. E. Arends, M. Pellizon, R. A. Sheldon, *Stud. Surf. Sci. Catal.* **1997**, 110, 1031.
- [8] K. H. Thompson, J. H. McNeill, C. Orvig, *Chem. Rev.* **1999**, 99, 2561.
- [9] Y. Shechter, J. Li, J. Meyerovitch, D. Gefel, R. Bruck, G. Elberg, D. S. Miller, A. Shisheva, *Mol. Cell Biochem.* **1995**, 153, 39.
- [10] H. V. Strout, P. P. Vicario, R. Saperstein, E. E. Slater, *Endocrinology* **1989**, 124, 1918.
- [11] S. W. Taylor, B. Kammerer, E. Bayer, *Chem. Rev.* **1997**, 97, 333.
- [12] M. Weyand, H.-J. Hecht, M. Kieß, M.-F. Liaud, H. Vilter, D. Schomburg, *J. Mol. Biol.* **1999**, 293, 595.
- [13] A. Messerschmidt, L. Prade, R. Wever, *Biol. Chem.* **1997**, 378, 309.
- [14] S. Macedo-Ribeiro, W. Hemrika, R. Renirie, R. Wever, A. Messerschmidt, *J. Biol. Inorg. Chem.* **1999**, 4, 209.
- [15] R. R. Eady, *Chem. Rev.* **1996**, 96, 3013.
- [16] M. Zhang, M. Zhou, R. L. van Etten, C. V. Stauffacher, *Biochemistry* **1997**, 36, 15.
- [17] J. E. Banabe, L. A. Echegoyen, B. Pastrona, M. Martinez-Maldonado, *J. Biol. Chem.* **1987**, 262, 9555.
- [18] W. Tsagkalidis, D. Rehder, *J. Biol. Inorg. Chem.* **1996**, 1, 507.
- [19] W. Tsagkalidis, D. Rodewald, D. Rehder, *Inorg. Chem.* **1995**, 34, 1943.
- [20] H. B. ten Brink, A. Tuynman, H. L. Dekker, W. Hemrika, Y. Izumi, T. Oshiro, H. E. Shoemaker, R. Wever, *Inorg. Chem.* **1998**, 37, 6780.
- [21] M. A. Andersson, S. G. Allenmark, *Tetrahedron* **1998**, 54, 15293.
- [22] H. Schmidt, M. Bashirpoor, D. Rehder, *J. Chem. Soc., Dalton Trans.* **1996**, 3865.
- [23] C. Bolm, F. Bienewald, *Angew. Chem. Int. Ed. Engl.* **1995**, 34, 2883.
- [24] K. Nakajima, K. Kojima, J. Fujita, *Bull. Chem. Soc. Jpn.* **1990**, 63, 2620.
- [25] D. C. Crans, C. M. Simone, *Biochemistry* **1991**, 30, 6734.
- [26] C. R. Cornman, T. C. Stauffer, P. D. Boyle, *J. Am. Chem. Soc.* **1997**, 119, 5986.
- [27] A. J. Tasiopoulos, A. T. Vlahos, A. D. Keramidas, T. A. Kabanos, Y. G. Deligiannakis, C. P. Raptopoulos, A. Terzis, *Angew. Chem. Int. Ed. Engl.* **1996**, 35, 2531.
- [28] S. C. Sendlinger, J. R. Nicholson, E. B. Lobkovsky, J. C. Huffman, D. Rehder, G. Christou, *Inorg. Chem.* **1993**, 32, 204.
- [29] K. K. Nanda, E. Sinn, A. W. Addison, *Inorg. Chem.* **1996**, 35, 2.
- [30] S. C. Davies, D. L. Hughes, Z. Janas, L. B. Jerzykiewicz, R. L. Richards, J. R. Sanders, J. E. Silverston, P. Sobota, *Inorg. Chem.* **2000**, 39, 3485.
- [31] H. Sakurai, H. Watanabe, H. Tamura, H. Yasui, R. Matsushita, J. Takada, *Inorg. Chim. Acta* **1998**, 283, 175.
- [32] D. X. West, S. B. Padhye, P. B. Sonawane, R. C. Chikate, *Asian J. Chem. Rev.* **1990**, 1, 125.
- [33] M. E. Hossain, M. N. Alam, M. A. Ali, M. Nazimuddin, F. E. Smith, R. C. Hynes, *Polyhedron* **1996**, 15, 973.
- [34] W. Banske, E. Ludwig, E. Uhlemann, F. Weller, K. Dehnicke, W. Herrmann, *Z. Anorg. Allg. Chem.* **1992**, 613, 36.
- [35] C. Weidemann, W. Pribsch, D. Rehder, *Chem. Ber.* **1989**, 122, 235.
- [36] D. Rehder, in: *Transition Metal NMR* (vol. 13 of *Studies in Inorganic Chemistry*; Ed.: P. S. Pregosin), Elsevier, Amsterdam, **1991**, p. 1.
- [37] D. Rehder, C. Weidemann, A. Duch, W. Pribsch, *Inorg. Chem.* **1988**, 27, 584.

- [38] A. J. Tasiopoulos, A. N. Troganis, A. Evangelou, C. R. Raptopoulou, A. Terzis, Y. Deligiannakis, T. A. Kabanos, *Chem. Eur. J.* **1999**, 5, 910.
- [39] M. E. Hossain, M. N. Alam, M. A. Ali, M. Nazimuddin, F. E. Smith, R. C. Hynes, *Polyhedron* **1996**, 15, 973.
- [40] G. R. Hanson, Y. Sun, C. Orvig, *Inorg. Chem.* **1996**, 35, 6507.
- [41] D. X. West, Y. Yang, T. L. Klein, K. I. Goldberg, A. E. Liberta, J. Valdes-Martinez, R. A. Toscano, *Polyhedron* **1995**, 14, 1681.
- [42] Z. Lu, C. White, A. L. Rheingold, R. H. Crabtree, *Inorg. Chem.* **1993**, 32, 3991.
- [43] P. Souza, A. I. Matesanz, V. Fernandez, *J. Chem. Soc., Dalton Trans.* **1996**, 3011.
- [44] J. Valdez-Martinez, R. A. Toscano, A. Zentella-Dehesa, M. M. Salberg, G. A. Brain, D. X. West, *Polyhedron* **1996**, 15, 427.
- [45] M. Soriano-Garcia, J. Valdés-Martínez, R. A. Toscano, J. Gómez-Lara, *Acta Crystallogr. C* **1985**, 41, 500.
- [46] G. Argay, A. Kálmán, V. M. Leovac, V. I. Cesljevic, B. Ribar, *J. Coord. Chem.* **1996**, 37, 165.
- [47] M. Farahbakhsh, H. Nekola, H. Schmidt, D. Rehder, *Chem. Ber./Recueil* **1997**, 130, 1129.
- [48] P. R. Klich, A. T. Daniher, P. R. Challen, D. B. McConville, W. J. Youngs, *Inorg. Chem.* **1996**, 35, 347.
- [49] H. Maeda, K. Kanamori, H. Michibata, T. Tonno, K. Okamoto, J. Hidaka, *Bull. Chem. Soc. Jpn.* **1993**, 66, 790.
- [50] N. V. Gerbeleu, I. F. Burshtein, G. A. Kiosse, I. G. Filippova, O. A. Bologa, V. I. Lozan, T. I. Malinovskii, *Dokl. Akad. Nauk SSSR* **1985**, 284, 155.
- [51] H. Schmidt, D. Rehder, *Inorg. Chim. Acta* **1998**, 267, 229.
- [52] V. Vergopoulos, S. Jantzen, N. Julien, E. Rose, D. Rehder, *Z. Naturforsch. B* **1994**, 49, 1127.
- [53] D. Rehder, C. Schulzke, H. Dau, C. Meinke, J. Hanss, M. Epple, *J. Inorg. Biochem.* **2000**, 80, 115, and literature cited therein.
- [54] M. Bashirpoor, H. Schmidt, C. Schulzke, D. Rehder, *Chem. Ber./Recueil* **1997**, 130, 651.
- [55] H. Tietz, K. Schmetlick, G. Kreisel, *Z. Chem.* **1985**, 25, 290.
- [56] G. M. Sheldrick, *SHELXS 86*, University of Göttingen, **1986**.
- [57] G. M. Sheldrick, *SHELXL 93*, University of Göttingen, **1993**.
- [58] S. Purohit, A. P. Koley, L. S. Prasad, P. T. Manoharan, S. Ghosh, *Inorg. Chem.* **1989**, 28, 3735.
- [59] M. Busch, M. Starke, *J. Prakt. Chem.* **1916**, 93, 59.

Received September 13, 2000
[I00344]